Physica Medica 148 (2026) 105833

Contents lists available at ScienceDirect

Physica Medica

journal homepage: www.elsevier.com/locate/ejmp

Original paper

Occupational radiation doses in CT-guided interventions: A multicentre evaluation with special emphasis on lung biopsies and eye lens doses

Hemmo Hartikainen [a,b,c,*], Antti Pekkarinen [b], Touko Kaasalainen [a], Mika Kortesniemi [a]

[a] HUS Diagnostic Center, Radiology, Helsinki University and Helsinki University Hospital, Haartmaninkatu 4, 00290 Helsinki, Finland
[b] Department of Medical Physics, The Wellbeing Services County of Kymenlaakso, Kymenlaakso Central Hospital, Kotkantie 41, 48210 Kotka, Finland
[c] Department of Physics and Astronomy, University of Turku, Finland

ARTICLE INFO

Keywords:
Dosimetry
CT-guided interventions
Biopsy

ABSTRACT

Purpose: This study aimed to investigate eye lens and whole-body radiation doses received by interventional radiologists during CT-guided procedures, with a particular focus on lung biopsies.
Methods: Simultaneous measurements of eye lens dose equivalent $H_p(3)$, deep-dose equivalent $H_p(10)$, and shallow-dose equivalent $H_p(0.07)$ were conducted under clinical conditions during CT-guided procedures in five Finnish hospitals during four separate four-week measurement periods. $H_p(3)$ was measured using EYE-D thermoluminescent dosimeters, while $H_p(10)$ and $H_p(0.07)$ were recorded using DIS-1 dosimeters. The $H_p(3)/H_p(10)$ and $H_p(3)/H_p(0.07)$ ratios, and $H_p(3)$ to dose-length product (DLP) were analysed to assess whether routinely measured quantities can provide a rough indication of eye lens dose in CT-guided procedures. The doses per CT procedure were analysed for all aforementioned dose equivalents to evaluate the annual exposures. Dosimeter calibration and quality control were performed at a secondary standard dosimetry laboratory. Staff positioning, radiation protection practices, and procedural variables were explored in relation to differences in observed exposure levels across hospitals and procedures.
Results and conclusions: Occupational radiation exposure during CT-guided procedures were generally negligible when appropriate radiological practices and protective equipment were used. One hospital showed significantly higher dose values due to the primary use of fluoroscopy and absence of a lead glass screen. Despite this aberrant result, exposure levels remained below annual occupational dose limits in all hospitals. Routinely measured $H_p(10)$ and $H_p(0.07)$ showed a strong relationship with $H_p(3)$ in the measurable dose data, suggesting that they may provide a rough indication of the order of magnitude of eye lens dose.

1. Introduction

Occupational radiation exposure is an essential concern in interventional radiology and image-guided procedures, where medical personnel are frequently exposed to scattered radiation. A key parameter for assessing radiation exposure to the eye lens is the personal dose.

equivalent $H_p(3)$ [1], which quantifies the dose at a 3 mm tissue depth and is particularly relevant in estimating eye lens radiation dose and consequential risk. Recent studies have demonstrated that radiation-induced cataracts can occur at lower doses than previously recognised. The International Commission on Radiological Protection (ICRP) has revised the threshold for cataract formation from 2 Gy (Gy) to 0.5 Gy [2] and there is on-going discussion whether the cataract formation should be considered also as a stochastic risk [3]. Consequently, the ICRP now recommends an occupational equivalent dose limit for the eye lens of 20 mSv (mSv) per year, averaged over five years, with no single year exceeding 50 mSv [4]. There have been studies with cases where the limit of 20 mSv and even the limit of 50 mSv have been exceeded [5–7]. A previous study in Finnish hospitals reported on the possibility, although unlikely, of interventional radiologists exceeding the single year eye dose limit of 50 mSv [8]. There is also evidence of cataract formation at even lower doses than 0.5 Gy [9]. These findings highlight the importance of monitoring and minimising eye lens exposure in interventional radiology and computed tomography (CT)-guided procedures where ionising radiation is routinely used.

CT-guided procedures, such as biopsies, rely on three primary imaging modes: spiral (helical), sequential (axial), and fluoroscopy [10]. Spiral imaging acquires continuous data as the patient table moves

* Corresponding author at: Department of Physics and Astronomy, University of Turku, Finland.
E-mail address: hemmo.p.hartikainen@utu.fi (H. Hartikainen).

https://doi.org/10.1016/j.ejmp.2026.105833
Received 20 July 2025; Received in revised form 12 April 2026; Accepted 3 June 2026
Available online 13 June 2026

through the CT gantry, creating a volumetric dataset that can be reconstructed in any plane or slice thickness. This provides a detailed three-dimensional representation of the target anatomical location, allowing operators to plan the procedure, visualise the target area from multiple angles, and verify the success of the procedure. Spiral scanning is typically used in the trajectory planning stage, where the access route for the instrument is decided. During the acquisition of'high dose' spiral images, the operator and staff typically remain outside the procedure room, resulting in negligible occupation exposure. After a needle or a probe is placed on the patient, it is guided towards the lesion using either sequential or fluoroscopy imaging mode. In brief, sequential and fluoroscopy modes correspond to a single rotation around the patient to track the needle/probe. The sequential, or"step-and-shoot", imaging acquires a predefined number of images (based on total collimation and detector configuration used) once x-rays are triggered by the radiologist in the CT scan room. During the acquisition of sequential images, the operator should be situated behind a lead glass shield or protective barrier to minimise radiation exposure. CT fluoroscopy offers real-time imaging and is used, for example, when precise biopsy needle placement or continuous monitoring is required. It may be especially beneficial when targeting the needle e.g. into moving lung lesions. During CT fluoroscopy, the operator often remains close to the patient to manually advance or adjust the needle under visual guidance. This proximity, combined with the patient acting as a source of scattered radiation and limited shielding options, may increase radiation exposure to the operator, particularly to the hands and eyes.

Previous studies on occupational exposure during CT-guided procedures have shown that operator doses, particularly to the eye lens, depend on the imaging mode used and the available radiation protection. In CT-guided biopsies performed with CT fluoroscopy and limited shielding, physician eye lens doses of the order of tens of microsieverts per procedure have been reported, with substantially higher values in some cases [11,12]. In contrast, when sequential imaging is used and the operator remains behind a protective lead screen, staff doses may remain very low, even below the detection limit [13]. These findings indicate that staff exposure in CT-guided procedures is highly dependent on local workflow and protection practices. At the same time, the available literature remains limited, particularly regarding direct $H_p(3)$ measurements collected during routine clinical work, supporting the need for further investigation of eye lens doses in CT-guided procedures.

Despite growing interest in eye lens doses, $H_p(3)$ is not commonly measured in routine occupational dosimetry. Instead, $H_p(10)$ or $H_p(0.07)$, which represent the personal dose equivalent at a 10-mm or 0.07-mm tissue depth, respectively, are often used to approximate $H_p(3)$ in practical applications [14]. However, using deep-dose equivalent, $H_p(10)$, or shallow-dose equivalent, $H_p(0.07)$, as surrogates for $H_p(3)$ can introduce uncertainties, as these quantities do not always correlate well, particularly under varying radiation exposure geometries and scattering conditions (different body shapes and postures, and varying x-ray spectra and beam geometries), which can result in different doses to different parts of the body [7]. Accurately measuring $H_p(3)$ presents several challenges due to the complexity of radiation scattering, variations in procedural techniques, exposure geometries, applied structural and personal radiation protection, and the positioning of occupational dosimeters [8,14–16]. Thermoluminescent dosimeters (TLDs) and optically stimulated luminescent dosimeters (OSLs) are commonly used for $H_p(3)$ monitoring [17].

In this study, $H_p(3)$, $H_p(0.07)$, and $H_p(10)$ measurements were conducted in five Finnish hospitals to assess occupational radiation exposure during various CT-guided procedures, with a primary focus on CT-guided lung biopsies and eye lens doses. The goal was to analyse these personal dose equivalents across different hospitals and procedures, identifying variations associated with specific procedures and hospital practices. Additionally, the aim was to investigate the relationships between $H_p(3)$ and the routinely recorded $H_p(10)$, $H_p(0.07)$, and dose length product (DLP) of a CT procedure, using simultaneous measurements to assess whether these quantities may provide a rough indication of the order of magnitude of eye lens dose. This research contributes to the development of improved radiation protection protocols and enhances occupational safety in medical imaging environments.

2. Materials and Methods

2.1. Measurements at the hospitals

Personal dose equivalents including $H_p(3)$, $H_p(0.07)$, and $H_p(10)$ were measured in five Finnish hospitals (H1, H2, H3, H4, and H5) during four separate four-week monitoring periods. Radiation doses from CT-guided lung biopsies were collected from H1, H2, H3, and H4. At H1, doses from CT-guided abdominal biopsies were also measured. At H5, instead of lung biopsies, doses from CT-guided bone biopsies were collected because the hospital does not perform lung biopsies. Doses from all *other CT-guided procedures* were also measured in every hospital. These generally include procedures that are less commonly performed at the hospitals, such as various other biopsies targeted to kidneys, liver, and lymph nodes as well as different types of CT-guided drainages.

The dosimeters used in the CT procedures measuring $H_p(10)$, and $H_p(0.07)$ were direct ion storage (DIS-1) dosimeters (Mirion Technologies (RADOS), Turku, Finland). $H_p(3)$ was measured with EYE-D thermoluminescent dosimeters (TLDs) [18] (RadCard, Poland). Background doses in each hospital were measured by storing one DIS-1 and two EYE-D dosimeters in the shielded control rooms, where the occupational group dosimeters were also stored when not in use. All hospitals used Siemens' CT-device models Somatom Definition Edge or Somatom X. Cite (Siemens Healthineers, Erlangen, Germany) except for H3, where GE Revolution HD CT-device (GE Healthcare, Milwaukee, Wisconsin, USA) was used.

The group dosimeters were worn by the interventional radiologists. DIS-1 dosimeters were worn either at chest level above the protective apron next to the official personal dosimeters or attached to the lowest middle part of the thyroid collar. The EYE-D dosimeters were attached to the side of the protective glasses or to a headband, i.e. approximately at eye level over the temple. The EYE-D dosimeter was always worn on the side towards the radiation source where the received dose is potentially higher. All participants wore a protective thyroid shield and an apron. Moreover, in all locations except H4, a movable lead glass screen was routinely used by radiologists when a sequential scan mode was used during procedures. During an original spiral imaging scan, the radiologists were not in the CT room but stayed in the control room. The only case when the radiologists should have been exposed to radiation without the movable lead screen was during fluoroscopy imaging, when the biopsy needle must be guided using real-time imaging.

Each hospital was given a form to document the procedure type, date, patient number, volumetric CT dose index ($CTDI_{vol}$), DLP, applied tube voltage, radiation protection used, positioning of staff in the CT room, and other essential observations. The DLP and $CTDI_{vol}$ values from fluoroscopy and sequence imaging, during which the radiologist was in the CT room, were later collected from Siemens Teamplay (Siemens Healthineers, Erlangen, Germany) dose monitoring system.

2.2. Positioning of interventional radiologist during CT-guided procedures

Fig. 1 shows the positions (G, F, and L) of the interventional radiologist during CT-guided procedures. The patient is positioned on the CT table (P), while the procedure is performed by the interventional radiologist. The position of the interventional radiologists relative to the CT gantry and patient varied somewhat across procedures, radiologists, and centres. For lung biopsies, the radiologist typically used sequential scanning mode (i-sequence) and stayed behind a movable protective lead shield (position L) at a distance of approximately 1.8–2.5 m from the CT scanner isocentre. In this position, the CT gantry provides

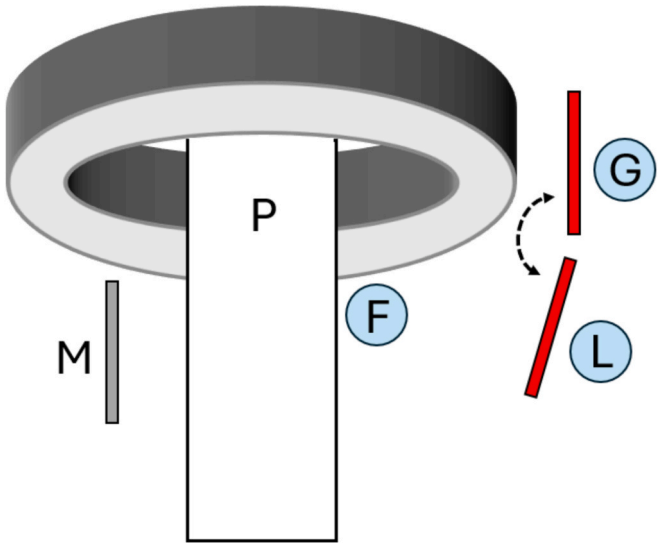

Fig. 1. Positions of interventional radiologists during various CT-guided procedures. The positions behind only the protective lead shield (L), the shield moved to the side of the gantry (G), as well as the position next to the patient (F) on the CT table (P) during fluoroscopy are shown. Also, the position of the ceiling-mounted monitor (M) is shown.

additional protection against scattered radiation from the patient. At the centre (H5) performing bone biopsies and *other procedures*, the radiologist stayed at a similar distance (1.8–2.5 m) behind the lead glass shield positioned more on the side of the CT gantry (position G) which together provide maximal shielding. When CT fluoroscopy mode (i-fluoro) was used, the radiologist stayed closer to the patient (position F), at approximately 0.5 m, and did not use the movable lead shield during exposures. A ceiling-mounted monitor (M) allowed continuous visualisation of imaging during procedures. For interventions performed on the contralateral side of the patient's body, the setup was mirrored relative to the arrangement shown in the figure.

2.3. Dosimetry

The $H_p(3)$ measurements were done using EYE-D dosimeters with LiF:Mg,Cu,P (MCP-N) TLDs [19]. The measurements were read at a national secondary standard dosimetry laboratory (SSDL) using an automatic TLD reader RE-2000 (Mirion Technologies (RADOS) Oy, Turku, Finland). Since the measurements could only be done in the SSDL, an additional exchange pair for each EYE-D dosimeter was used to make the transition between study periods more seamless. The calibration of the TLDs from raw pulse counts to $H_p(3)$ at the SSDL were performed separately for the two dosimeter groups using N80 radiation quality [20]. The radiation quality was chosen to best fit the characteristics of the scattering radiation arriving to the dosimeters during a procedure. Its mean photon energy (~65 keV) is close to the energy range (100—120 kV) used for lung biopsies and *other procedures* in this study. Bone biopsies were performed with tube voltages between 100 and 140 kV, most commonly at 130–140 kV.

The calibrations were performed using a 20 cm x 20 cm water-filled cylindrical PMMA phantom. The TLDs were calibrated with doses of 20, 50, 100, 200, 1000, and 2000 μSv. Three dosimeters were used per dose point. Three background dosimeters were placed in the control room for background measurement. A linear fit was applied to the dose and pulse data using the background-subtracted mean pulse count from the three dosimeters from each dose group to establish calibration factors. The uncertainty for the calibration was measured to be 3 % for the first calibration and 4 % for the second. The calculation was based on the maximum deviation of the mean value (three dosemeters) of each dose group from the linear response. The uncertainty of the linearity of the dose response was calculated to be 7 % for the first calibration and 3 % for the second, based on the maximum deviation of the $H_p(3)$ value of the mean value of each dose group on the linear fit compared at the nominal dose of each group.

Repeatability of measurements and the homogeneity of the used TLDs were tested before the first study period at the SSDL using IR-2000 (Mirion Technologies (RADOS) Oy, Turku, Finland) which uses Sr-90 as a radiation source. All TLDs were irradiated and read three times. The maximum deviation of an individual TLD from its mean response was 5 %, representing the repeatability uncertainty. The variation in the mean pulse count averaged over the three irradiations for all 46 TLDs was 4 %, which was taken as the uncertainty of batch homogeneity. The uncertainty for the background reduction was estimated to be 6 % based on the deviations of the mean values within each group of background dosemeters. The estimation included a total of six background dosimeters used in the calibrations and the eight used in each hospital over the four measurement periods. The minimum detectable signal was calculated as three times the standard deviation of the detected pulse count from zero dose TLDs [21]. This translates to a minimum detectable dose (MDD) of 9 μSv for $H_p(3)$ using the calibrations explained before.

Energy response and the angle dependency were not tested. Previous measurements with the same EYE-D dosimeters and TLDs with ISON80-N250 X-ray qualities and Cs-137 have reported an uncertainty of 2 % for the energy response [8]. For the lower photon energies relevant to scattered CT radiation, this uncertainty is expected to be higher. The angle dependency was reported to be 7 % for angles between 0° and 60° using the same qualities. The fading of the dosimeters was 5 %, given by the manufacturer leading to a maximum of 0.5 % loss of collected doses during the measurement periods. The combined and expanded ($k = 2$) uncertainty of all beforementioned uncertainties was ± 24 % for both calibrations.

The DIS-1 dosimeters were read at the hospitals using calibrated DBR-2 reader units (Mirion Technologies (RADOS) Oy, Turku, Finland). The doses recorded by the radiologists' dosimeters were adjusted by subtracting the background doses measured at each hospital. The dosimeters were calibrated at the accredited dosimetric service company (Doseco Oy, Jyväskylä, Finland). According to the manufacturer, the applicable dose range of DIS-1 dosimeter is from 1 μSv to 1 Sv for $H_p(10)$, and from 10 μSv to 1 Sv for $H_p(0.07)$. The lower limits of these ranges are used as the MDD values for given dose equivalents. The expanded uncertainty ($k = 2$) for the calibration accuracy is given as ± 5 % at 1 mSv (Cs-137) for $H_p(10)$ and ± 10 % at 10 mSv (Cs-137). The expanded uncertainty ($k = 2$) is reported to be ± 30 % for both $H_p(10)$ and $H_p(0.07)$ in the energy ranges of 15 keV – 9 MeV and 6 keV and higher, respectively. The uncertainty for the angular response is given to be ± 20 % up to 60° at 65 keV for both dose values. Calculating the combined expanded uncertainty gives ± 37 % for $H_p(10)$ and ± 38 % for $H_p(0.07)$.

2.4. Statistical methods and data presentation

Personal dose equivalents $H_p(10)$, $H_p(0.07)$, and $H_p(3)$ are presented as cumulative values collected during each measurement period. For each procedure type, the corresponding medians and expanded uncertainties were calculated and presented for these quantities. The average patient dose, expressed as the DLP, is reported as the mean per-procedure value for each procedure type across all hospitals and measurement periods. Only scans acquired while the radiologist was present in the room were included in the DLP calculations, excluding the routinely performed spiral scans at the beginning and end of the procedures. For DLP, dispersion across measurement periods was summarised for each hospital and procedure category using the per-procedure mean values at the period level, and results are reported as the mean and standard deviation.

Descriptive statistics were used to support the analysis of relationships between measured dose equivalents and eye lens dose. Linear

regression (Microsoft Excel, linear least squares fit) and Spearman's rank correlation were used to examine relationships between $H_p(10)$, $H_p(0.07)$, and $H_p(3)$, with the latter chosen to assess monotonic relationships without assuming linearity or normally distributed data. The expanded uncertainty (~95 % confidence interval, k = 2) for the regression of the slope was calculated from the combined uncertainties of these dose equivalents and the standard error of the fit. Nonparametric tests were used because the sample sizes were small, uneven, and normal distribution could not be assumed. The Kruskal-Wallis test was applied for comparisons involving more than two groups (e.g. all hospitals), and the Mann-Whitney *U* test for comparisons between two groups (e.g. lung biopsies versus other procedures). Results are reported as p-values, with $p < 0.05$ considered statistically significant. Statistical analyses were performed using Python (ver. 3.9.) with the pandas and SciPy libraries. In all statistical analyses, doses below the detection limit were replaced with the corresponding MDD. For per-procedure dose calculations and annual dose estimates, only procedure types and measurement periods with notable cumulative doses were included.

3. Results

The procedure types, their numbers, measured total $H_p(10)$, $H_p(0.07)$, and $H_p(3)$ values (above personal protective equipment), and the average per-procedure DLP values for all hospitals from every measurement period are shown in Table 1. Radiation protection setups typical for each centre and procedure type were used. No *other procedures* were conducted in H1 or H3 during the measurement periods. Thus, these categories are not shown in the table. In H2, all *other procedures* were abdominal cavity drainages. In H4, these procedures included a wider variety including biopsies of lymph nodes, liver, groin, and kidneys. Also, a single drainage of pelvic abscess was performed. H5 performed brachytherapy, nerve root blocks, and one procedure each of myelography and sclerotherapy. All doses in H4 during the first and fourth period were from single lymph node and kidney biopsies, respectively. Between-period dispersion of per-procedure DLPs (mean ± SD, mGy cm) were: H1 lung biopsy 105 ± 5 and H1 abdominal biopsy 89 ± 34; H2 lung biopsy 104 (single period) and H2 abdominal cavity drainage 141 ± 14; H3 lung biopsy 235 ± 20; H4 lung biopsy 96 ± 9 and H4 other procedures 666 ± 301; H5 bone biopsy 52 ± 10 and H5 other procedures 171 ± 212.

The only notable, meaning clearly above MDD, for $H_p(10)$, $H_p(0.07)$, and $H_p(3)$ doses for lung biopsies were from all four measurement periods at H4 and from the second period at H1. Additionally, the only notable doses for *other CT-guided procedures* were again from all measurement periods at H4. Any other procedure type in other hospitals did not have notable doses leading to the comparison of $H_p(3)$ to $H_p(10)$ and $H_p(0.07)$ being done using only the nine values from lung biopsies and *other procedures*. The relationship between $H_p(3)$ and $H_p(0.07)$ using the nine dose pairs is shown in Fig. 2a with a linear fit. The linear fit gives the dependency between the doses as $H_p(3) = (0.75 \pm 0.35) \cdot H_p(0.07)$, with a coefficient of determination of $R^2 = 0.97$. The relationship between $H_p(3)$ and $H_p(10)$ is similarly shown in Fig. 2b. The linear fit gives a very similar relationship of $H_p(3) = (0.69 \pm 0.31) \cdot H_p(10)$, with $R^2 = 0.97$. The relationship between $H_p(0.07)$ and $H_p(10)$ was $H_p(0.07) = (0.92 \pm 0.49) \cdot H_p(10)$ with $R^2 = 0.999$. Spearman's rank correlation confirmed strong monotonic associations between the nine dose pairs, with $\rho = 0.88$ ($p = 0.002$) for $H_p(3)$ versus $H_p(10)$, $\rho = 0.82$ ($p = 0.006$) for $H_p(3)$ versus $H_p(0.07)$, and $\rho = 0.98$ ($p < 0.001$) for $H_p(0.07)$ versus $H_p(10)$, supporting the use of a linear fit between these quantities.

The $H_p(3)$ values per DLP, the number and types of procedures, and the $H_p(10)$, $H_p(0.07)$, and $H_p(3)$ per procedure are shown in Table 2. The values in the table have been calculated for the periods and procedure types during which the doses were notable. No procedures were marked for *other procedures* at H4 during the second study period, but noticeable doses were read from both the EYE-D and DIS-1. The $H_p(10)$, $H_p(0.07)$, and $H_p(3)$ per lung biopsy procedure were similar across all measurement periods (N = 23) at H4 with total averages of 50 ± 20, 45 ± 20, and 39 ± 10 μSv per procedure, respectively. The same values at H1 during the second period (N = 23) were just 2.5 ± 1, 2.2 ± 0.9, and 3.2 ± 0.8 μSv per procedure. The average values for $H_p(10)$, $H_p(0.07)$, and $H_p(3)$ for *other procedures* (N = 5) at H4 were 360 ± 140, 342 ± 130, and 260 ± 70 μSv per procedure, respectively. The average values for $H_p(3)$ per DLP for lung biopsies were 2.35 ± 1 μSv/(mGycm) at H4 and 0.68 ± 0.2 μSv/(mGycm) at H1. The same value for *other procedures* at H4 was 0.65 ± 0.4 μSv/(mGycm).

At H4, 96 % of the CT-guided lung biopsies and 100 % of other CT-guided biopsies were performed by one radiologist. Taking the average value of the $H_p(3)$ per procedure and multiplying the value by the average number of procedures each measurement period and approximating the year having 13 4-week study periods (52 weeks) gives a cumulative annual $H_p(3)$ estimate of 3000 ± 800 μSv for lung biopsies for the individual radiologist. The annual estimate for *other procedures* for the same radiologist was calculated similarly, except for the second period with no procedures registered, giving an estimate of 6500 ± 2000 μSv. Similarly, the annual estimates for $H_p(10)$ and $H_p(0.07)$ for lung biopsies are 3700 ± 1400 and 3400 ± 1300 μSv, respectively. The same values for *other procedures* are 5900 ± 2200 and 5600 ± 2200 μSv. At

Table 1
Procedure types, number of procedures, total $H_p(10)$, $H_p(0.07)$, and $H_p(3)$ values, and average per-procedure DLP from four separate four-week measurement periods at each hospital. The expanded uncertainties for $H_p(10)$, $H_p(0.07)$, and $H_p(3)$ are 37 %, 38 %, and 24 %, respectively. Upper-bound totals indicate the MDD when values were below detection (1 μSv for $H_p(10)$, 10 μSv for $H_p(0.07)$, and 9 μSv for $H_p(3)$). Radiation protection systems typical for each centre were in place. All $H_p(d)$ doses were measured above personal protective equipment.

Procedure	1st / 2nd / 3rd / 4th measurement period				
	N	Hp(10) [μSv]	Hp(0.07) [μSv]	Hp(3) [μSv]	Average DLP [mGy cm]
H1					
Lung biopsy	11 / 23 / 8 / 9	1 / 57 / 1 / 1	10 / 50 / 10 / 20	9 / 73 / 9 / 9	100 / 108 / 110 / 101
Abdominal biopsy	1 / 1 / 0 / 0	5 / 2 / 3 / 1	20 / 10 / 10 / 10	9 / 9 / 9 / 9	65 / 113 / 0 / 0
H2					
Lung biopsy	0 / 0 / 0 / 3	5 / 1 / 1 / 1	20 / 10 / 30 / 10	11 / 9 / 9 / 9	0 / 0 / 0 / 104
Abdominal cavity drainage	1 / 2 / 1 / 1	3 / 1 / 1 / 1	10 / 10 / 10 / 10	9 / 9 / 9 / 9	148 / 138 / 155 / 123
H3					
Lung biopsy	5 / 5 / 2 / 0	4 / 1 / 1 / 2	20 / 10 / 10 / 50	9 / 12 / 9 / 14	256 / 233 / 217 / 0
H4					
Lung biopsy	8 / 6 / 3 / 6	242 / 312 / 151 / 434	200 / 280 / 150 / 400	309 / 214 / 128 / 251	88 / 93 / 95 / 109
Other procedures	1 / 0 / 3 / 1	300 / 49 / 1243 / 229	280 / 50 / 1150 / 230	251 / 42 / 832 / 161	548 / 0 / 746 / 428
H5					
Bone biopsy	13 / 12 / 8 / 12	6 / 2 / 1 / 6	20 / 10 / 10 / 10	9 / 9 / 9 / 9	66 / 50 / 48 / 43
Other procedures	3 / 0 / 2 / 3	2 / 3 / 1 / 1	30 / 10 / 10 / 20	9 / 9 / 9 / 9	246 / 0 / 512 / 48

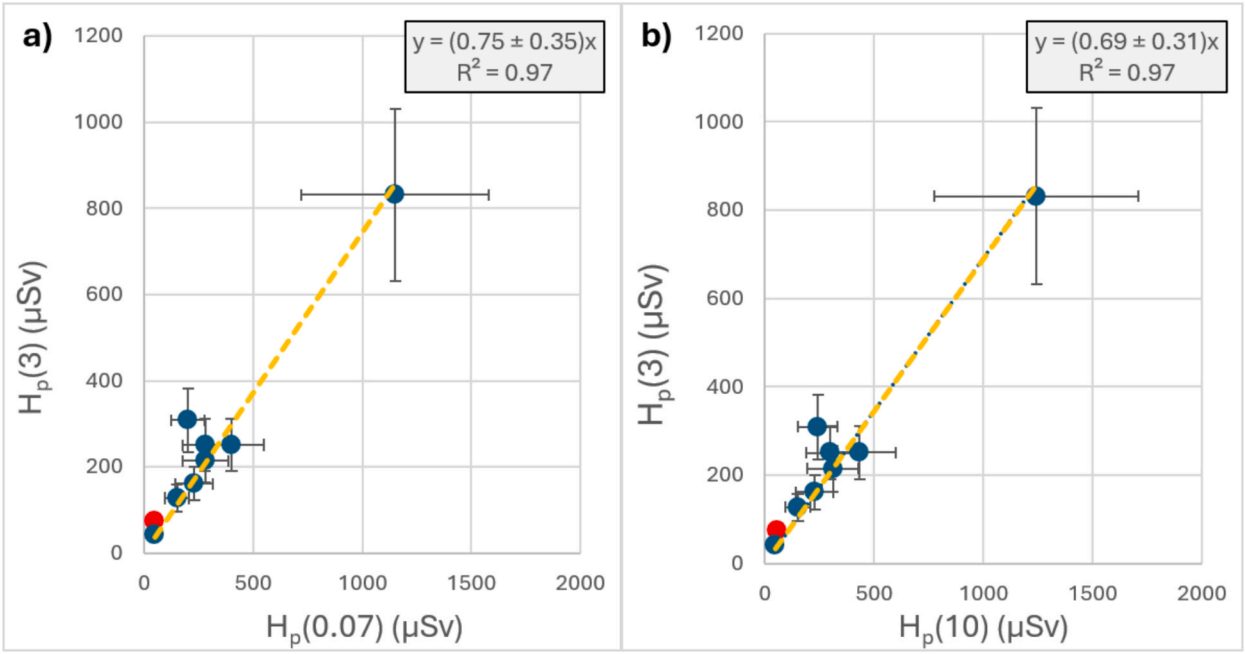

Fig. 2. A linear fit to show the relationship of $H_p(3)$ to $H_p(0.07)$ (a) and $H_p(10)$ (b). The error bars correspond to the expanded uncertainties of 24 %, 38 %, and 37 % for $H_p(3)$, $H_p(0.07)$, and $H_p(10)$, respectively. The intercept has been set to zero. Each dot represents the cumulative values of a four-week measurement period for a single procedure type and hospital. Blue dot represents hospital H4 and red H1. Radiation protection systems typical for each centre were in place. All $H_p(d)$ doses were measured above personal protective equipment. (For interpretation of the references to colour in this figure legend, the reader is referred to the web version of this article.)

Table 2
The hospitals, measurement periods, and procedure types along with the used imaging mode (fluoro/sequence), during which the measured $H_p(d)$ doses were clearly above MDD, as well as the number of procedures (N) and the $H_p(3)$ per DLP, and $H_p(10)$, $H_p(0.07)$, $H_p(3)$ per procedure. The expanded uncertainties for $H_p(10)$, $H_p(0.07)$, and $H_p(3)$ are 37 %, 38 %, and 24 %, respectively. Radiation protection systems typical for each centre were in place. All $H_p(d)$ doses were measured above personal protective equipment.

Hospital, period	Procedure type	N	$H_p(3)$/DLP (μSv/mGy cm)	$H_p(10)$/procedure (μSv)	$H_p(0.07)$/procedure (μSv)	$H_p(3)$/procedure (μSv)
H1, 2	Thorax (i-sequence)	23	0.68 ± 0.2	2.5 ± 1	2.2 ± 0.9	3.2 ± 0.8
H4, 1	Thorax (i-fluoro)	8	3.5 ± 0.9	30 ± 10	25 ± 10	39 ± 10
H4, 2	Thorax (i-fluoro)	6	2.3 ± 0.6	52 ± 20	47 ± 20	36 ± 9
H4, 3	Thorax (i-fluoro)	3	1.3 ± 0.4	50 ± 20	50 ± 20	43 ± 10
H4, 4	Thorax (i-fluoro)	6	2.3 ± 0.6	72 ± 30	67 ± 30	42 ± 10
H4, 1	Others (i-fluoro)	1	0.46 ± 0.2	300 ± 120	280 ± 110	250 ± 60
H4, 2	Others (i-fluoro)	0 [a)]	–	–	–	–
H4, 3	Others (i-fluoro)	3	1.1 ± 0.3	410 ± 160	383 ± 150	280 ± 70
H4, 4	Others (i-fluoro)	1	0.38 ± 0.1	229 ± 90	230 ± 88	160 ± 40

a) Zero procedures were marked.

H1, four radiologists performed lung biopsies during the second period. One radiologist performed 10 out of the 23 procedures while the others performed 8, 4, and 1 procedure(s). Extrapolating the annual $H_p(10)$, $H_p(0.07)$, and $H_p(3)$ values gives annual estimates of 330 ± 130, 290 ± 110, and 420 ± 100 μSv for the radiologist with the highest count of performed lung biopsies. The estimations were calculated using only one study period to give a conservative estimate since no notable doses were measured during other periods.

A global Kruskal–Wallis test for lung biopsies showed significant differences between hospitals for both $H_p(3)$/procedure ($p = 0.039$) and $H_p(10)$/procedure ($p = 0.045$). H2 was excluded for small sample size and H5 was excluded for not having any lung biopsies. Within the three hospitals tested, doses were statistically stable across measurement periods (all $p > 0.37$). In H4, *other procedures* delivered a five- to eightfold higher per-procedure dose than lung biopsies. However, Mann–Whitney tests gave p-values of 0.057 for both $H_p(3)$/procedure and $H_p(10)$/procedure, indicating no statistically significant difference between *other procedures* and lung biopsies in H4.

4. Discussion

In this study, we measured personal dose equivalents $H_p(10)$, $H_p(0.07)$, and $H_p(3)$ received by interventional radiologists during various CT-guided procedures, with particular emphasis on lung biopsies. We also investigated the relationships between $H_p(3)$ and DLP, $H_p(10)$, and $H_p(0.07)$ in order to assess whether routinely recorded quantities may provide a rough indication of eye lens dose.

The personal dose equivalents in CT-guided lung biopsies varied significantly across hospitals with $H_p(3)$ and $H_p(10)$ per procedure medians at H4 exceeding the low-dose hospital H1 by over a magnitude. A global Kruskal-Wallis test confirmed the difference across hospitals for both quantities. In contrast, doses remained statistically stable within hospitals across measurement periods, indicating that the observed differences are systematic rather than the result of short-term fluctuations. A comparison within H4 revealed that *other procedures* delivered a five- to eight-fold higher per procedure dose to staff than lung biopsies. Although the Mann-Whitney p-values for both values were 0.057,

narrowly missing the conventional p = 0.05 threshold, the dose difference is large and clinically meaningful.

The main differences in radiation protection and clinical practice between the departments were the use of movable lead screens and the selection of imaging modes (sequence vs. fluoroscopy). At Hospital 4, with significantly higher staff doses measured, fluoroscopy (i-fluoro with Siemens Somatom X.Cite) imaging mode was systematically used, which prevented radiologists from using a protective lead screen. In all other hospitals, a sequence scanning mode was mainly used during the procedures with only a few exceptions. This resulted in remarkably lower doses for the interventionalists.

In all hospitals, a scout scan and a spiral scan were performed prior to the procedure, during which the radiologist remained in the control room instead of the CT room. In all hospitals except H4, the radiologist primarily used sequential imaging mode during the procedure and stood behind a movable lead glass screen. Fluoroscopy imaging mode was employed only when real-time guidance of the biopsy needle was required, which was rare during routine lung biopsies in most centres. During fluoroscopy, positioning the lead glass screen between the radiation source (mainly scattered dose from a patient) and the radiologist is challenging, as the radiologist must stand close to the patient to guide the needle. At H4, however, fluoroscopy was the only imaging mode for needle guidance following the initial scout and spiral scans, both for lung biopsies and *other procedures*. According to our results, the lead glass screen plays a critical role in radiation protection in CT-guided biopsies. For N80 (65 keV) radiation quality, 0.5 mm Pb is generally expected to attenuate approximately 95 % of the primary beam. In the study by Dávila *et al.*, attenuation values above 99 % were reported for their specific experimental setup [22].

The relationships between $H_p(3)$ and $H_p(0.07)$ (Fig. 2a), and $H_p(3)$ and $H_p(10)$ (Fig. 2b) showed good correlation with coefficient of determination $R^2 = 0.97$ and Spearman's p-values well below 0.05 for both linear fits. This suggests that $H_p(10)$ and $H_p(0.07)$ may provide a rough indication of the order of magnitude of eye lens dose in CT-guided procedures. However, this observation should be interpreted with caution, because eight of the nine dose pairs used in the analysis originated from a single hospital, where most procedures were performed by the same radiologist. Therefore, the observed relationships should be considered exploratory and centre-dependent rather than general conversion equations for predicting Hp(3). The only data point from H1 included as many lung biopsies as all measurement periods at H4 combined. Also, the high-dose pair at H4 from the third period can influence the linear fit. Removing this value gives alternative linear equations of $H_p(3) = (0.81 \pm 0.40) \cdot H_p(0.07)$ with $R^2 = 0.91$ and $H_p(3) = (0.75 \pm 0.35) \cdot H_p(10)$ with $R^2 = 0.92$. However, the change is small relative to the associated uncertainty in the slope. Previous measurements done by Pekkarinen *et al.* reported a conversion equation of $H_p(3) = (0.53 \pm 0.45) \cdot H_p(10)$ with $R^2 = 0.96$ for interventional radiologists and cardiologists in Finnish hospitals [8].

Although the $H_p(3)$, $H_p(10)$, and $H_p(0.07)$ values at H4 were significantly higher than at any other hospital for both lung biopsies and *other procedures*, the mean per-procedure DLP (Table 1), reflecting patient radiation dose, were comparable to those in most other hospitals. This suggests that the use of fluoroscopy at H4 does not result in higher patient doses during routine lung biopsies. Interestingly, the highest patient doses for lung biopsies were found at H3, despite reported similarities in workflow and radiation protection practices across hospitals. This is likely to be due to a different CT scanner brand and model with related differences e.g. in scanner and exposure geometry, applied spectra and protocol parameters. In contrast, the DLP values for *other procedures* at H4 were considerably higher than those at other sites. This may be attributed to the inclusion of non-routine, complex procedures and the small sample size. For example, in the first measurement period at H4, a single lymph node biopsy accounted for the entire recorded DLP.

Literature shows only a few studies addressing eye lens doses of interventionists during CT-guided biopsies. Most published data focus on general IR procedures or IC procedures. A comparison of the reported operator eye lens doses from previous studies and the present study is shown in Table 3. Busoni *et al.* reported an $H_p(3)$ of 153 μSv per CT-guided lung biopsy when no suspended shield or protective eyewear was used [11]. In the present study, the average $H_p(3)$ per CT-guided lung biopsy was 39 ± 10 μSv at H4, and 3.2 ± 0.8 μSv during the second measurement period at H1. In all other hospitals and measurement periods, $H_p(3)$ values were close to background levels, effectively near zero. Inaba *et al.* reported an average eye lens dose of 40 μSv per procedure, with a maximum of 300 μSv per procedure for a physician performing CT-guided biopsies with fluoroscopy, without any radiation protections taken into account [12]. The average eye lens dose observed per lung biopsy at H4, where fluoroscopy was used exclusively, aligns closely with these findings. Additionally, the average $H_p(3)$ per *other CT-guided procedure* at H4 was 260 ± 70 μSv, which is consistent with the literature values given above. In contrast, the corresponding value at H1 was nearly 50 times lower than that reported by Busoni *et al.* and approximately 13 times lower than the average given by Inaba *et al.* A Finnish study by Kaartinen *et al.* observed that the personal dose equivalent values per CT-guided procedure were below the detection limit when the operator remained behind a lead screen during CT-guided procedures [13]. This aligns with the results of this study, where mostly no cumulative doses were observed at hospitals where the lead glass screen was routinely used. However, direct comparison with literature values should be approached with caution as differences in radiation protection arrangements, procedural protocols, and facility-specific working practices may significantly affect resulting dose levels.

The estimated annual $H_p(3)$ values for the two radiologists with the highest number of CT-guided procedures were approximately 10 mSv at H4 and 0.4 mSv at H1. These values remain below the annual dose limits of 50 mSv or cumulative limit of 100 mSv over five consecutive years (20 mSv/year on average) for the eye lens. Similarly, the estimated annual $H_p(10)$ and $H_p(0.07)$ doses were 10 mSv and 9 mSv, respectively, at H4 and 0.3 mSv for both quantities at H1. A conservative estimation of effective dose from $H_p(10)$ can be calculated by dividing the over-apron $H_p(10)$ by a factor of 30 [23], where the effective dose is defined as the sum of equivalent doses in all specified tissues and organs, each weighted by its tissue weighting factor. This factor has been used in interventional and CT-guided procedures as a practical approximation, reflecting the average attenuation provided by a 0.35–0.5 mm Pb aprons under typical scatter radiation conditions. Although the actual ratio between $H_p(10)$ and effective dose varies with X-ray energy, projection, and apron material, the use of 1/30 provides a conservative upper-bound estimate for most clinical scenarios. Thus, the annual effective doses using the aforementioned factor are 0.3 mSv at H4 and 0.01 mSv at H1. The estimated effective dose also remains below the annual dose limit. The approximations of annual dose do not account for additional procedures involving ionising radiation that were performed by the radiologists but not included in this study. As an example, the radiologist at H4 also performs angiography examinations, which were not included in this study. The primary contributors for the higher doses observed at H4 were likely differences in radiation protection practices and procedural workflow, as the average doses per procedure were significantly higher at H4 compared to H1.

All dose values reported in this study were measured outside the protective gear. Several studies have examined the dose reduction factor (DRF) of lead glasses in interventional radiology (IR) and interventional cardiology (IC) [7,24–26]. Morcillo *et al.* report DRFs of 1.2–1.3 for the left eye and 1.3–1.4 for the right eye [7]. One challenge in estimating DRF is the variation in lead glass designs, which offer differing levels of protection depending on the angle of exposure. For example, Haga *et al.* report a DRF of 2.5 for the left eye when using a wraparound design that offers better lateral protection for the eye lenses [26]. The angle of incident scatter radiation significantly affects the DRF, often leading to

Table 3
Comparison of reported operator eye lens doses in computed tomography (CT)-guided procedures from previous studies and the present study.

Study	Clinical setting	Dose metric	Reported eye lens dose	Protection/workflow
Busoni et al. [11]	CT-guided lung biopsy	Median $H_p(3)$ per procedure	153 μSv/procedure	No suspended shield or protective eyewear
Inaba et al. [12]	CT-guided interventions using multidetector CT fluoroscopy	Mean eye lens dose per procedure	39.1 ± 36.3 μSv/procedure	Fluoroscopy; no radiation protection taken into account
Kaartinen et al. [13]	CT-guided interventions	Personal dose equivalent per procedure	Below detection limit	Operator remained behind a lead screen
Present study, Hospital 4	CT-guided lung biopsy	Mean $H_p(3)$ per procedure	39 ± 10 μSv/procedure	Fluoroscopy used exclusively; no movable lead glass screen during exposure
Present study, Hospital 1 (second measurement period only)	CT-guided lung biopsy	Mean $H_p(3)$ per procedure	3.2 ± 0.8 μSv/procedure	Sequential imaging with protective lead screen
Present study, Hospital 4	Other CT-guided procedures	Mean $H_p(3)$ per procedure	260 ± 70 μSv/procedure	Fluoroscopy used; no movable lead glass screen during exposure
Present study, other hospitals / periods	CT-guided procedures	Cumulative $H_p(3)$	Close to background or below minimum detectable dose	Lead screen routinely used in sequential workflow

discrepancies between the left and right eye. The eye positioned closer to the radiation source usually receives a higher dose and has a lower DRF. It is also worth to discuss the positioning of the EYE-D and DIS-1 dosimeters. The EYE-D dosimeter was placed on the side of the head, while the DIS-1 dosimeter was generally worn on the chest level, making them perpendicular to each other. As a result, the EYE-D dosimeter was directed towards the gantry, whereas the DIS-1 was oriented towards the patient, who acts as a source of scattered radiation. This difference in orientation may influence the measured ratios between dose equivalents, since the dosimeters were exposed to somewhat different angular distributions of the scattered radiation field. In addition, partial shielding by the operator's body or protective equipment may have differed between dosimeter positions, which may contribute to the uncertainty of the comparisons.

This study has several limitations. First, the number of CT-guided procedures included was relatively small, partly due to lost dosimeters at H1, where the majority of CT-guided lung biopsies were performed. Second, data were collected during only four distinct measurement periods, and thus the number of measurement points was limited. Third, not all the procedures were properly documented, and in some cases, dosimeters were not worn. This discrepancy became apparent when comparing the number of procedures recorded in the Siemens Teamplay dose monitoring system with the manually completed user forms. Only the procedures documented on the forms were included in the dose analyses. This inconsistency may explain the recorded doses for *other CT-guided procedures* at H4 during the second measurement period, despite no procedures having been marked on the form. If a procedure was performed, but not documented, while dosimeters were worn, an overestimation of dose per procedure would result.

5. Conclusions

Occupational radiation exposure during CT-guided procedures remains negligible when appropriate protective equipment is used and radiation-safe working practices are followed. However, significantly higher $H_p(3)$, $H_p(10)$, and $H_p(0.07)$ values were observed at one centre, where a movable lead glass screen was not used and fluoroscopy (i-fluoro) was employed as the primary imaging mode instead of sequential imaging mode. Routinely measured $H_p(10)$ and $H_p(0.07)$ values showed a strong relationship with $H_p(3)$ during CT-guided lung biopsies and other procedures and may provide a rough indication of the order of magnitude of eye lens dose. However, the Hp(3) per DLP, and Hp(10), Hp(0.07), and Hp(3) per procedure differed by a factor of ten between hospitals, indicating that these relationships are not universally applicable across different clinical settings.

Declaration of competing interest

The authors declare that they have no known competing financial interests or personal relationships that could have appeared to influence the work reported in this paper.

Acknowledgements

Authors thank the staff of the CT-guided procedures in every hospital for participating in the study. The authors also acknowledge Carita Lindholm and Juha Suutari from STUK for aiding with the calibration and reading of the TLDs.

References

[1] Publication ICRP. 103 Protection Quantities and ICRU Report 39/51 Operational Quantities. J ICRU 2020;20:20–3. https://doi.org/10.1177/1473669120966212.
[2] Clement CH, editor. ICRP Publication 118. ICRP Statement on Tissue Reactions / Early and Late Effects of Radiation in Normal Tissues and Organs – Threshold Doses for Tissue Reactions in a Radiation Protection Context. vol. 41. Annals of the ICRP; 2012.
[3] Shore RE. Radiation and cataract risk: Impact of recent epidemiologic studies on ICRP judgments. Mutat Res Rev Mutat Res 2016;770:231–7. https://doi.org/10.1016/j.mrrev.2016.06.006.
[4] Clement CH, editor. ICRP Publication 139. Occupational Radiological Protection in Interventional Procedures. vol. 47. Annals of the ICRP; 2018.
[5] Merrachi NA, Bouchard-Bellavance R, Perreault P, Gilbert P, Soulez G, Bouchard L, et al. Eye lens dosimetry in interventional radiology: assessment with dedicated Hp (3) dosimeters. Can Assoc Radiol J 2020;72:1–7. https://doi.org/10.1177/0846537120911755.
[6] O'Connor U, Walsh C, Gallagher A, Dowling A, Guiney M, Ryan JM, et al. Occupational radiation dose to eyes from interventional radiology procedures in light of the new eye lens dose limit from the International Commission on Radiological Protection. Br J Radiol 2015;88:1–7. https://doi.org/10.1259/bjr.20140627.
[7] Morcillo AB, Alejo L, Huerga C, Bayón J, Marín A, Corredoira E, et al. Occupational doses to the eye lens in pediatric and adult noncardiac interventional radiology procedures. Med Phys 2021;48:1956–66. https://doi.org/10.1002/mp.14753.
[8] Pekkarinen A, Lindholm C, Kortesniemi M, Siiskonen T. Staff eye lens dose in interventional radiology and cardiology in Finland. Phys Med 2022;98:1–7. https://doi.org/10.1016/j.ejmp.2022.04.005.
[9] Ainsbury EA, Dalke C, Hamada N, Benadjaoud MA, Chumak V, Ginjaume M, et al. Radiation-induced lens opacities: Epidemiological, clinical and experimental evidence, methodological issues, research gaps and strategy. Environ Int 2021;146:1–14. https://doi.org/10.1016/j.envint.2020.106213.
[10] Jones KA, Dixon RG, Collins JD, Walser EM, Nikolic B. Best Practices guidelines for CT-Guided Interventional Procedures. JVIR 2017;29:22–4. https://doi.org/10.1016/j.jvir.2017.10.021.
[11] Busoni S, Bruzzi M, Giomi S, Poggiali C, Quattrocchi M, Betti M, et al. Surgeon eye lens dose monitoring in interventional neuroradiology, cardiovascular and radiology procedures. Phys Med 2022;104:123–8. https://doi.org/10.1016/j.ejmp.2022.11.002.
[12] Inaba Y, Hitachi S, Watanuki M, Chida K. Occupational radiation dose to eye lenses in CT-guided interventions using MDCT-fluoroscopy. Diagnostics 2021;11:1–9. https://doi.org/10.3390/diagnostics11040646.

[13] Kaartinen S, Husso M, Matikka H. Operator's eye lens dose in computed tomography-guided interventions. Eur Radiol 2020;31:4377–85. https://doi.org/10.1007/s00330-020-07576-0.
[14] Vanhavere F, Carinou E, Domienik J, Donadille L, Ginjaume M, Gualdrini G, et al. Measurements of eye lens doses in interventional radiology and cardiology: final results of the ORAMED project. Radiat Meas 2011;46:1243–7. https://doi.org/10.1016/j.radmeas.2011.08.013.
[15] Wickramasinghe SU, Ramanathan V, Sarasanandarajah S. Assessment of occupational eye lens dose in interventional cardiology suites in Sri Lanka. Phys Med 2024;127:1–11. https://doi.org/10.1016/j.ejmp.2024.104826.
[16] Principi S, Ginjaume M, Duch MA, Sánchez RM, Fernández JM, Vano E. Influence of dosemeter position for the assessment of eye lens dose during interventional cardiology. Radiat Prot Dosim 2015;164:79–83. https://doi.org/10.1093/rpd/ncu359.
[17] Suliman II. Review of various methods for occupational eye lens dosimetry in X-ray interventional procedures. Radiat Phys Chem 2025;236. https://doi.org/10.1016/j.radphyschem.2025.112936.
[18] Bilski P, Bordy JM, Daures J, Denoziere M, Fantuzzi E, Ferrari P, et al. The new EYE-D^{TM} dosemeter for measurements of HP(3) for medical staff. Radiat Meas 2011;46:1239–42. https://doi.org/10.1016/j.radmeas.2011.04.031.
[19] Olko P, Budzanowski M, Bilski P, Milosevic S, Obryk B, Ochab E, et al. Application of MCP-N (LiF:Mg,Cu,P) TL detectors in monitoring environmental radiation. Nucl Technol Radiat Protect 2004;19:20–5. https://doi.org/10.2298/ntrp0401020o.
[20] Ferrari P, Mariotti F, Campani L, Castelluccio DM, Pierotti L, Pettinato C, et al. First results of an eye lens dosimetry survey in an interventional cardiology department. J Radiol Prot 2015;35:467–72. https://doi.org/10.1088/0952-4746/35/2/467.
[21] Fernández SDS, García-Salcedo R, Mendoza JG, Sánchez-Guzmán D, Rodríguez GR, Gaona E, et al. Thermoluminescent characteristics of LiF:Mg,Cu,P and $CaSO_4$:Dy for low dose. measurement 2016. https://doi.org/10.1016/j.apradiso.2016.02.011.
[22] Dávila HO, Díaz Merchán JA, Vega Carrillo HR, Martínez Ovalle SA. Assessment of the effectiveness of attenuation of Pb aprons by using TLD dosimetry and Monte Carlo calculations. Appl Radiat Isot 2018;138:56–9. https://doi.org/10.1016/j.apradiso.2017.05.012.
[23] Siiskonen T, Tapiovaara M, Kosunen A, Lehtinen M, Vartiainen E. Monte Carlo simulations of occupational radiation doses in interventional radiology. Br J Radiol 2007;80:460–8. https://doi.org/10.1259/bjr/26692771.
[24] Vanhavere F, Carinou E, Gualdrini G, Glairand I, Sans Merce M, Ginjaume M, et al. ORAMED: optimization of radiation protection of medical staff. EURADOS 2012.
[25] Magee JS, Martin CJ, Sandblom V, Carter MJ, Almén A, Cederblad A, et al. Derivation and application of dose reduction factors for protective eyewear worn in interventional radiology and cardiology. J Radiol Prot 2014;34:811–23. https://doi.org/10.1088/0952-4746/34/4/811.
[26] Haga Y, Chida K, Kaga Y, Sota M, Meguro T, Zuguchi M. Occupational eye dose in interventional cardiology procedures. Sci Rep 2017;7:1–7. https://doi.org/10.1038/s41598-017-00556-3.